This article has been accepted for publication in a future issue of this journal, but has not been fully edited. Content may change prior to final publication. Citation information: DOI 10.1109/TCSII.2016.2621772, IEEE Transactions on Circuits and Systems II: Express Briefs

A 0.3-V 1-μW Super-Regenerative Ultrasound Wake-Up Receiver with Power Scalability

Hiroshi Fuketa, Shinichi O'uchi, and Takashi Matsukawa, *Member, IEEE*

***Abstract*—This brief presents an ultra-low power wake-up receiver using ultrasound for IoT applications. To achieve both high sensitivity and low power consumption, we propose a Colpitts-oscillator-based super-regenerative receiver (COSR). Owing to the simple architecture of the proposed COSR, a lowest supply voltage operation of 0.3 V and a smallest area are achieved. Furthermore, the power consumption of the proposed wake-up receiver is scalable and is determined by the input signal sensitivity and data rate, which are configurable by the user. In a field test, the proposed wake-up receiver consumes 1 μW, which is smaller by 77% than that of a conventional ultrasound wake-up receiver at a comparable communication distance and data rate.**

***Index Terms*—Super-regenerative, ultrasound, ultra-low power, ultra-low voltage, wake-up receiver**

I. Introduction

RECENTLY, distributed wireless sensor devices for IoT (Internet of Things) applications have been drawing much attention. In these devices, ultra-low power operation is strongly required to mitigate maintenance costs such as battery replacement. A wake-up receiver is a promising technique that can significantly reduce the power consumption of wireless sensor nodes, since a power-hungry RF circuit can be almost always turned off by using the wake-up receiver [1-6].

Although many RF-based wake-up receivers consume more than 10 μW [1,2], Milosiu *et al.* proposed a 3 μW wake-up receiver [3]. Another low-power wake-up receiver was demonstrated in [4] and it achieves 116-nW operation at a cost of low sensitivity. Compared with such RF-based technique, an optical technique can dramatically reduce power consumption (695pW) [5], whereas the light must be focused on the receiver chip to attain a communication distance of more than 1 m. Thus, this optical technique is not practical for actual IoT devices. To increase the communication distance with moderate power, a wake-up receiver using ultrasound was proposed in [6], and a communication distance of 8.6 m was achieved.

In this brief, we propose a wake-up receiver using ultrasound. Fig. 1 illustrates the system overview assumed in this brief. The advantages of the ultrasound wake-up system are as follows: 1) There are a few interference signals over a range of ultrasound frequencies in typical environments [6], and 2) built-in speakers in laptops and smartphones can emit low-frequency ultrasound waves [7,8], which implies that these devices have the potential to act as hosts of wireless nodes with low implementation costs. In the proposed receiver, a super-regenerative technique is applied. Owing to its simple architecture, a lowest supply voltage (V_{DD}) of 0.3 V and a smallest area can be achieved compared with conventional wake-up receivers. The measurement results show that the power dissipation of the proposed wake-up receiver depends on the data rate and input signal sensitivity, which can be configured by user-defined parameters such as clock period and duty cycle. Finally, we demonstrate in a field test that the proposed receiver consumes 1 μW, which is smaller by 77% than that of a conventional ultrasound receiver at a comparable communication distance and data rate.

Manuscript received August 16, 2016; revised October 14, 2016.

The authors are with Nanoelectronics Research Institute, National Institute of Advanced Industrial Science and Technology (AIST), Ibaraki 305-8568, Japan (e-mail: h-fuketa@aist.go.jp).

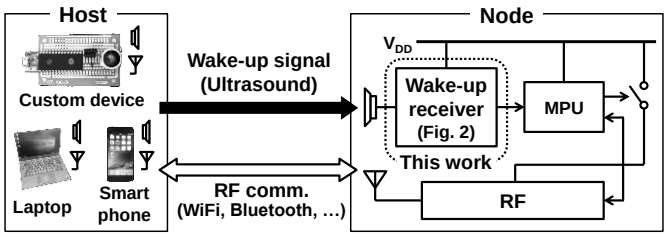

Fig. 1. Block diagram of the system assumed in this work. A power-hungry RF circuit can be almost always turned off by using a wake-up receiver.

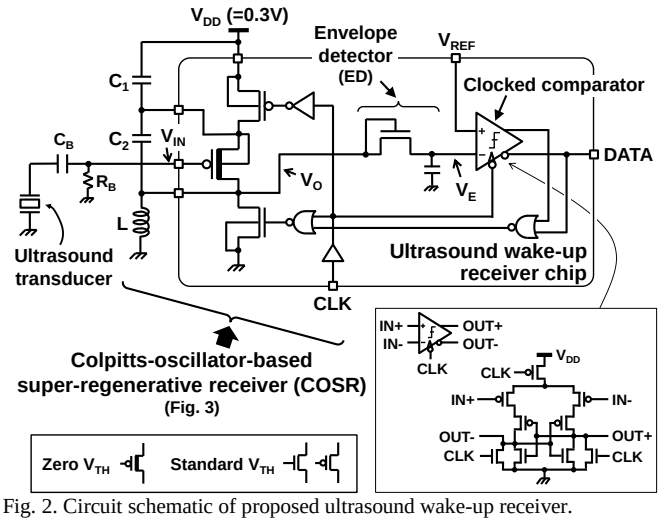

Fig. 2. Circuit schematic of proposed ultrasound wake-up receiver.

II. Circuit Description

Fig. 2 shows a circuit schematic of the proposed ultrasound wake-up receiver. The receiver operates at V_{DD}=0.3V.

This article has been accepted for publication in a future issue of this journal, but has not been fully edited. Content may change prior to final publication. Citation information: DOI 10.1109/TCSII.2016.2621772, IEEE Transactions on Circuits and Systems II: Express Briefs

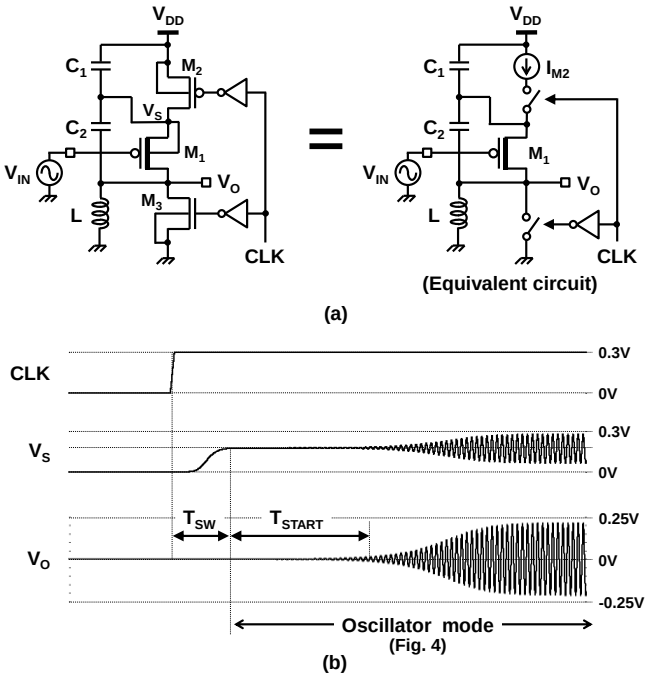

Fig. 3. (a) Circuit schematic of proposed Colpitts-oscillator-based super-regenerative receiver (COSR) and its equivalent circuit. COSR forms a common-gate Colpitts oscillator with an enable signal (CLK). (b) Simulated waveform of COSR (COSR operates as an independent oscillator, for reference). V_S denotes the source voltage of M_1.

A. Colpitts-Oscillator-Based Super-Regenerative Receiver

Various super-regenerative receivers have been proposed to achieve both high sensitivity and low power consumption for RF receivers [9,10]. Bohorquz *et al.* proposed a super-regenerative receiver with an RF antenna incorporated into an oscillator [9]. However, this circuit topology optimized for an RF antenna is not suitable for an ultrasound receiver. In [10], an antenna is connected to a low noise amplifier (LNA). This circuit technique can be adopted for the ultrasound receiver, whereas LNA must be implemented, which makes it difficult to operate at an ultra-low voltage.

In this brief, we propose a Colpitts-oscillator-based super-regenerative receiver (COSR). The circuit schematic is shown in Fig. 3(a). A common-gate Colpitts oscillator that utilizes a zero-V_{TH} transistor to achieve ultra-low voltage operation is proposed in [11]. In the proposed COSR, two transistors M_2 and M_3 are added to the Colpitts oscillator to realize super-regenerative operation. A zero-V_{TH} transistor is usually available in commercial foundry technologies [12]. M_2 is used to quench the oscillator, as indicated in the equivalent circuit in Fig. 3(a). Fig. 3(b) shows the waveform of COSR. When CLK is low, the Colpitts oscillator is disabled. By contrast, when CLK is high, the oscillator is enabled and begins oscillating ("oscillator mode"). Since the startup time of the oscillator T_{START} depends on the amplitude of the input signal V_{IN} (which will be explained later in Section II-B), COSR can demodulate amplitude-modulated signals. M_3 in Fig. 3(a) is used to rapidly stop the oscillation, which can improve the maximum data rate. Since M_2 and M_3 have standard V_{TH}, the leakage current of COSR is significantly reduced when the oscillator is disabled, which enables low-power operation.

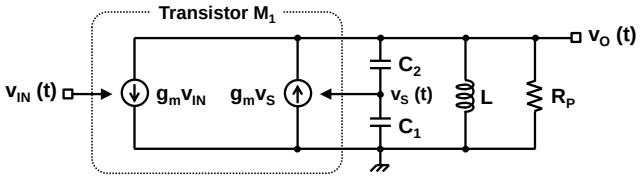

Fig. 4. Small-signal equivalent circuit of COSR during oscillator mode [Fig. 3(b)].

B. Startup time of COSR

In this section, the dependence of the oscillator startup time T_{START} on the amplitude of the input signal V_{IN} in the proposed COSR is analytically derived based on [9,13]. As shown in Fig. 3(b), T_{SW} is defined as the time from when CLK is asserted until the transistor M_2 starts operating as a current source. Startup time T_{START} is defined as the period in which the amplitude of V_O reaches a certain reference voltage V_{REF}. Fig. 4 illustrates the small-signal equivalent circuit of COSR during the oscillator mode shown in Fig. 3(b). In Fig.4, $v_{IN}(t)$ and $v_O(t)$ represent the input and output signals of COSR (V_{IN} and V_O in Fig. 3) in the time domain, respectively. In the frequency domain, the relation between v_{IN} and v_O can be written by using the Laplace variable s as

$$-g_m V_{IN}(s) + g_m V_S(s) = \left(sC + \frac{1}{sL} + \frac{1}{R_P}\right) V_O(s)\,, \quad (1)$$

$$V_S(s) = \frac{C_1}{C_1+C_2} V_O(s)\,, \quad (2)$$

$$C = \frac{C_1 C_2}{C_1+C_2}\,, \quad (3)$$

where $V_{IN}(s)$ and $V_O(s)$ are the Laplace transforms of $v_{IN}(t)$ and $v_O(t)$, respectively, g_m is the transconductance of the transistor M_1, and R_P is the parasitic resistance of the inductor L. Here, we assume that the output resistances of M_1 and M_2 are large enough to be ignored for simplicity. From (1)-(3), the output of COSR can be expressed as

$$V_O(s) = \frac{-Z_0\omega_0 s}{s^2+2\zeta\omega_0 s+{\omega_0}^2} \cdot g_m V_{IN}(s)\,, \quad (4)$$

$$\zeta = \frac{Z_0}{2R_P}\left(1 - \frac{C_1}{C_1+C_2} g_m R_P\right), \quad (5)$$

where ω_0 and Z_0 are the resonant frequency and impedance of the resonant tank [13], respectively, and they are given by

$$\omega_0 = 1/\sqrt{LC}\,, \quad (6)$$

$$Z_0 = \sqrt{L/C}\,. \quad (7)$$

When v_{IN} is sinusoidal and its frequency coincides with the resonant frequency ω_0, it can be expressed as

$$v_{IN}(t) = V_{IN} \sin \omega_0 t\,. \quad (8)$$

From (4) and (8), the output of COSR is approximated as

$$v_O(t) \approx \frac{Z_0 g_m V_{IN}}{2\zeta\sqrt{1-\zeta^2}} e^{-\zeta\omega_0 t} \sin\sqrt{1-\zeta^2}\,\omega_0 t\,. \quad (9)$$

From the definition of T_{STRAT}, the amplitude of V_O reaches V_{REF} at t=T_{STRAT}. That is, T_{STRAT} is given by

$$|v_O(t = T_{START})| \approx \frac{Z_0 g_m V_{IN}}{2|\zeta|\sqrt{1-\zeta^2}} e^{-\zeta\omega_0 T_{START}} = V_{REF}\,. \quad (10)$$

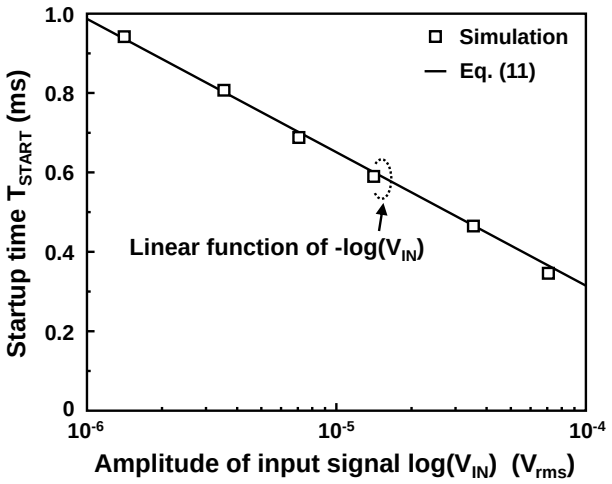

Fig. 5. Simulated and calculated T_{START} as a function of V_{IN} when V_{REF} is 10mV.The frequency of V_{IN} coincides with the resonant frequency of COSR.

Therefore, T_{STRAT} can be expressed as

$$T_{START} = -\alpha \ln V_{IN} + T_0 \,, \tag{11}$$

where

$$\alpha = \frac{1}{-\zeta\omega_0} > 0 \,, \tag{12}$$

$$T_0 = \frac{1}{-\zeta\omega_0} \ln\left(\frac{2|\zeta|\sqrt{1-\zeta^2}}{Z_0 g_m} V_{REF}\right). \tag{13}$$

To verify the correctness of (11), the calculated T_{START} is compared with the simulated results in Fig. 5. Eq. (11) indicates that T_{START} is a linear function of –log(V_{IN}), which is consistent with the simulated results, as shown in Fig. 5.

C. Circuit Behavior of Wake-Up Receiver

In this section, the circuit behavior of the proposed wake-up receiver shown in Fig. 2 is explained. Fig. 6 shows the simulated waveform of the receiver. The input signal of the receiver (V_{IN}) is modulated using on-off-keying (OOK). In this simulation, the amplitude of V_{IN} is 20 μV_{rms}, and V_{REF} is 10 mV. T_H represents the period in which CLK is high and here T_H is set to

$$T_H = T_{START} + T_{SW} + T_{ED} \,, \tag{14}$$

where T_{ED} is the delay time of the envelope detector (ED). In this paper, the diode rectifier is used for ED (Fig. 2). T_{ED} of the diode-rectifier ED is 0.2 ms, whereas the start-up time (T_{START}+ T_{SW}) is 0.9 ms at V_{IN}=20μV_{rms}. This means that T_{START}+ T_{SW} is dominant in (14) and hence the performance of the ED is not a critical issue.

When the amplitude of V_{IN} is larger than 20 μV_{rms}, COSR starts oscillating and the amplitude of the output signal of ED (V_E in Fig 2) reaches V_{REF} within T_H. In this case, the demodulated signal (DATA) becomes high by comparing V_E with V_{REF} at the negative edge of CLK. On the other hand, if the amplitude of V_{IN} is less than 20 μV_{rms}, V_E does not reach V_{REF} within T_H, and hence DATA remains low. This means that the OOK-modulated signal, whose amplitude is larger than 20 μV_{rms}, can be successfully demodulated, as shown in Fig. 6.

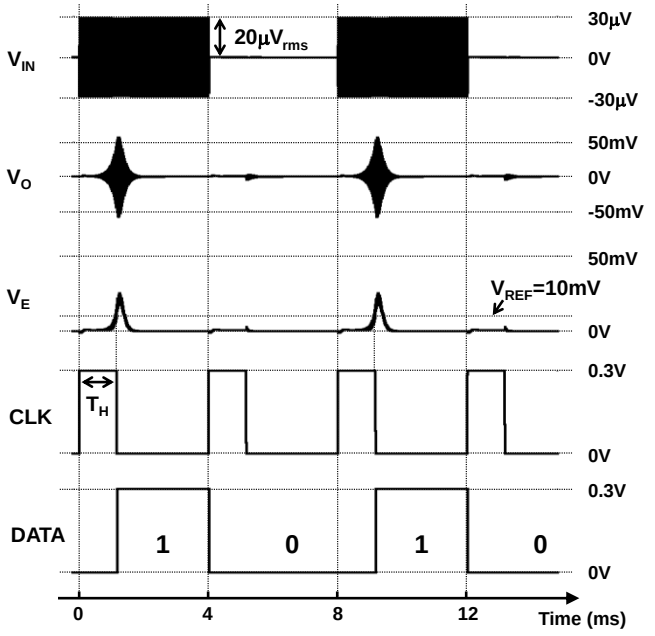

Fig. 6. Simulated waveform of proposed wake-up receiver (Fig. 2). The input signal (V_{IN}) is modulated using OOK and its amplitude is 20 μVrms.

Here, P_{RX} is defined as the power dissipation of the proposed receiver. P_{RX} is given by

$$P_{RX} = \frac{T_{CLK}-T_H}{T_{CLK}} P_L + \frac{T_H}{T_{CLK}} P_H \,, \tag{15}$$

where T_{CLK} is the clock period, and P_L and P_H are the power consumption of the receiver when CLK is low and high, respectively.

The proposed COSR consumes a large portion of the total power of the receiver. Thus, P_H is expressed as

$$P_H \approx \frac{V_{DD}}{T_H} \int_0^{T_H} I_{M2}(t)\, dt \,, \tag{16}$$

where $I_{M2}(t)$ is the current of transistor M_2 in COSR [Fig. 3(a)] assuming that CLK is asserted at t=0. P_H is much larger than P_L; hence P_{RX} in (15) is approximated as

$$P_{RX} \approx \frac{T_H}{T_{CLK}} P_H = f_{CLK} V_{DD} \cdot \int_0^{T_H} I_{M2}(t)\, dt \,, \tag{17}$$

where f_{CLK} is the clock frequency (= data rate). The transistor M_2 operates as a constant current source at t>T_{SW}, as shown in Fig. 3(b). Therefore, (17) can be rewritten as

$$P_{RX} \approx f_{CLK} V_{DD} \left(\int_0^{T_{SW}} I_{M2}(t)\, dt + (T_H - T_{SW}) I_{M2} \right)$$

$$= f_{CLK} V_{DD} \left(T_H I_{M2} + \int_0^{T_{SW}} I_{M2}(t)\, dt - T_{SW} I_{M2} \right) \tag{18}$$

$$= f_{CLK} V_{DD} (-\alpha\, I_{M2} \log V_{IN} + Q) \,, \tag{19}$$

where

$$I_{M2} = I_{M2}(t = T_{SW}) \,, \tag{20}$$

$$Q = \int_0^{T_{SW}} I_{M2}(t)\, dt + (T_0 + T_{ED}) I_{M2} \,. \tag{21}$$

The minimum amplitude of V_{IN}, that is, the sensitivity of the input signal, can be determined by T_H since T_{START} depends linearly on –log(V_{IN}) as indicated in (11). If a higher sensitivity

This article has been accepted for publication in a future issue of this journal, but has not been fully edited. Content may change prior to final publication. Citation information: DOI 10.1109/TCSII.2016.2621772, IEEE Transactions on Circuits and Systems II: Express Briefs

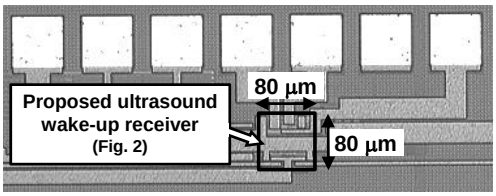

Fig. 7. Die photograph of proposed ultrasound wake-up receiver.

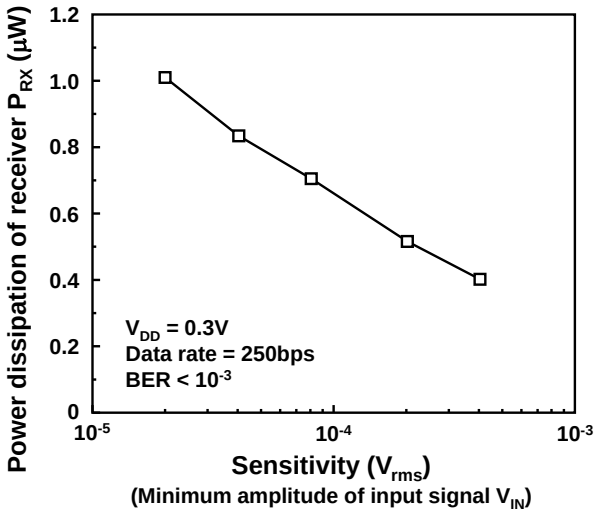

Fig. 8. Measured power dissipation of proposed wake-up receiver as a function of input signal sensitivity. P_{RX} linearly depends on $-\log(V_{IN})$.

is required, T_H must be increased, which results in a rise in P_{RX}, as indicated in (18). By contrast, P_{RX} can be reduced if the required sensitivity is low. Furthermore, (18) indicates that P_{RX} is proportional to the data rate (= f_{CLK}). This means that P_{RX} depends on the sensitivity and data rate that are determined by T_H and f_{CLK}, respectively.

III. Experimental Results

The proposed wake-up receiver circuit was fabricated in a 250 nm CMOS process. A die photograph is shown in Fig. 7. The proposed receiver occupies 80 x 80 μm^2. In this brief, the carrier frequency of ultrasound wake-up signals is chosen as 41 kHz, which is almost equal to the resonant frequency of the ultrasound transducers used in this work (UT1612MPR and UR1612MPR [14]). The off-chip capacitors (C_1 and C_2 in Fig. 2) and inductor (L in Fig. 2) of COSR are set to 3.5 nF and 10 mH, respectively, so that the oscillation frequency of COSR coincides with the carrier frequency of the ultrasound signals.

First, the dependences of the power dissipation of the proposed wake-up receiver on the sensitivity and data rate are measured. In these measurements, the signal generated by a function generator is directly input to the proposed receiver (V_{IN} in Fig. 2), and the bit error rate (BER) is kept at less than 10^{-3}. Fig 8 shows the measured power dissipation of the receiver (P_{RX}) at a data rate of 250 bps as a function of the minimum amplitude of V_{IN} (that is, sensitivity). This figure indicates that the measured P_{RX} increases as V_{IN} is reduced and is nearly a linear function of $-\log(V_{IN})$. This is consistent with (19). Fig. 9 illustrates the measured dependence of P_{RX} on the data rate when the sensitivity is 20 μV_{rms}. For this sensitivity,

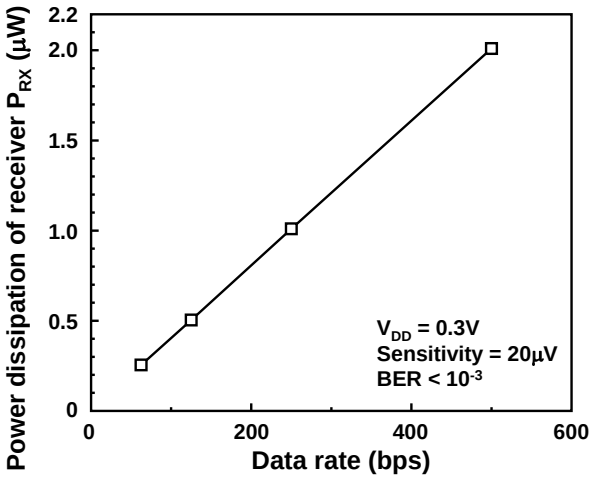

Fig. 9. Measured power dissipation of proposed wake-up receiver as a function of data rate. P_{RX} is proportional to the data rate.

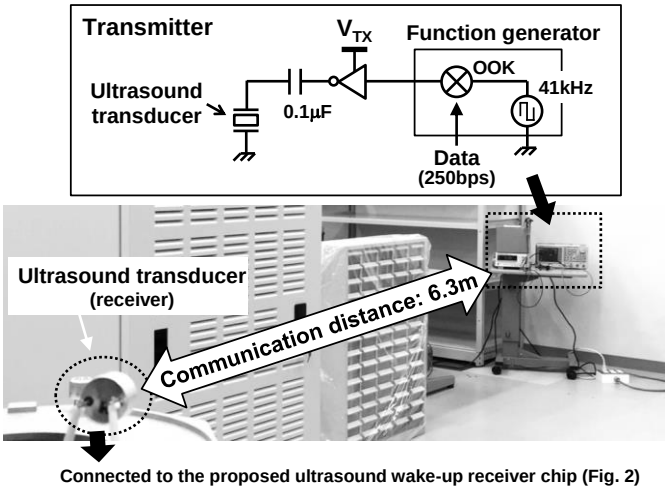

Fig. 10. Setup of field test using ultrasound.

the maximum data rate is 500 bps. The measured P_{RX} is proportional to the data rate (=f_{CLK}), which is also consistent with (19).

Next, we show the measurement results of the field test using an ultrasound. The test setup is shown in Fig. 10. In this setup, the communication distance is 6.3 m, and we use C_B and R_B (Fig. 2) of 0.1 μF and 10 kΩ, respectively. In the transmitter of the ultrasound, a 41-kHz square wave is generated and modulated using OOK by a function generator, as illustrated in the inset of Fig. 10. Fig. 11 shows the measured power consumption of the receiver (P_{RX}) as a function of that of the transmitter (P_{TX}). P_{TX} is controlled by changing the supply voltage of the buffer in the transmitter (V_{TX} in the inset of Fig. 10), and is calculated from the difference between the power consumption of the buffer with and without the ultrasound transducer. The receiver consumes 1 μW to achieve a communication distance of 6.3 m while keeping BER < 10^{-3} when P_{TX} is 1 mW. Fig. 11 indicates that P_{RX} depends on P_{TX}, since the amplitude of the ultrasound waves grows as P_{TX} increases. Therefore, when P_{TX} is increased to 17 mW, P_{RX} can be reduced to 610 nW.

Finally, the proposed wake-up receiver is compared with the

This article has been accepted for publication in a future issue of this journal, but has not been fully edited. Content may change prior to final publication. Citation information: DOI 10.1109/TCSII.2016.2621772, IEEE Transactions on Circuits and Systems II: Express Briefs

TABLE I COMPARISON WITH CONVENTIONAL WAKE-UP RECEIVERS

	ESSCIRC13 [3]	CICC13 [4]	CICC12 [5]	JSSC13 [6]	This work
Transmit method	RF (868 MHz)	RF (2.4 GHz)	Optical	Ultrasound (40.6 kHz)	Ultrasound (41 kHz)
CMOS process (nm)	130	130	65	180	250
Supply voltage V_{DD} (V)	2.5	1.2 / 0.5	1.2	0.6	0.3 ✓
Maximum data rate (bps)	8192	31k	91	250	500
Signal sensitivity	-83 dBm ($16\ \mu V_{rms}$)*1	-41 dBm ($2.0\ mV_{rms}$)*1	NA	$20\ \mu V_{rms}$	$20\ \mu V_{rms}$
Power consumption	8 μW (@ 256bps)	116 nW	695 pW	4.4 μW (@ 250bps)	-77% → 1 μW (@ 250bps)
Communication distance	Estimated *2		Measured		
	53 m (Tx: 1.0 mW)	1.1 m (Tx: 1.0 mW)	< 1m (Tx: 0.5W LED)	8.6 m (Tx: 16 mW)	6.3 m (Tx: 1.0 mW) ✓
Power scalability	Yes (Data rate)	NA	NA	NA	Yes (Data rate & sensitivity) ✓
Area (mm^2)	2.72	0.35	0.01	1.24	0.0064 ✓

(*1) 50Ω impedance is assumed. (*2) Isotropic and lossless antennas with path-loss exponent of 3 are assumed [4].

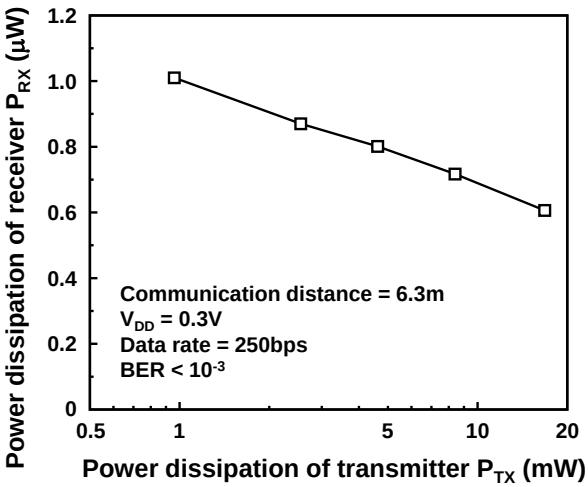

Fig. 11. Measured power dissipations of receiver and transmitter in the field test with ultrasound frequency of 41 kHz.

conventional receivers in Table I. The proposed COSR achieves high signal sensitivity even without LNA. Owing to the simple architecture of COSR, the proposed wake-up receiver can operate at a lowest V_{DD} of 0.3 V, and its area is the smallest among the conventional receivers. The power consumption of COSR is 1 μW, which is smaller by 77% than that of a conventional ultrasound wake-up receiver at an identical sensitivity of 20 μV_{rms} and data rate of 250 bps [6]. Although the power consumption of the receiver proposed in this work is larger than in previous works [4,5], the proposed receiver can communicate over a longer distance. In addition, the power consumption of the proposed receiver is scalable and is determined by the data rate and sensitivity, which are configurable by the user. In a field test, the Tx and Rx power consumption of the proposed receiver are smaller by 93% and 77%, respectively, than that of a conventional receiver [6] at a comparable distance and data rate.

IV. CONCLUSIONS

In this brief, a super-regenerative wake-up receiver was presented. The proposed receiver achieved a lowest V_{DD} of 0.3V and a smallest area among conventional wake-up receivers owing to the simple architecture of the proposed COSR. The measurement results showed that the power dissipation of the proposed receiver depends on the sensitivity and data rate, that is, the proposed receiver has power scalability. In a field test using ultrasound, we demonstrated that the proposed receiver consumes 1 μW, which is smaller by 77% than that of a conventional ultrasound wake-up receiver at a comparable communication distance and data rate.

REFERENCES

[1] S. Moazzeni, et al., "An Ultra-Low-Power Energy-Efficient Dual-Mode Wake-Up Receiver," *IEEE Trans. Circuits Syst. I*, vol. 62, no. 2, pp. 517–525, Feb. 2015.

[2] H. Cho, et al., "A 37.5 μW Body Channel Communication Wake-Up Receiver With Injection-Locking Ring Oscillator for Wireless Body Area Network," *IEEE Trans. Circuits Syst. I*, vol. 60, no. 5, pp. 1200–1208, May 2013.

[3] H. Milosiu, et al., "A 3-μW 868-MHz Wake-Up Receiver with -83 dBm Sensitivity and Scalable Data Rate," *Proc. ESSCIRC*, pp. 387–390, 2013.

[4] S. Oh, et al., "A 116nW Multi-Band Wake-Up Receiver with 31-bit Correlator and Interference Rejection," *Proc. CICC*, pp. 1–4, 2013.

[5] G. Kim, et al., "A 695 pW Standby Power Optical Wake-up Receiver for Wireless Sensor Nodes," *Proc. CICC*, pp. 1–4, 2012.

[6] K. Yadav, et al., "A 4.4-μW Wake-Up Receiver Using Ultrasound Data," *IEEE J. Solid-State Circuits*, vol. 48, no. 3, pp. 649–660, Mar. 2013.

[7] H. Lee, et al., "Chirp Signal-Based Aerial Acoustic Communication for Smart Devices," *Proc. INFOCOM*, pp. 2407–2415, 2015.

[8] M. Hanspach and M. Goetz, "On Covert Acoustical Mesh Networks in Air," *Journal of Communications*, vol. 8, no. 11, pp. 758–767, Nov. 2013.

[9] J. Bohorquez, et al., "A 350 μW CMOS MSK Transmitter and 400 μW OOK Super-Regenerative Receiver for Medical Implant Communications," *IEEE J. Solid-State Circuits*, vol. 44, no. 4, pp. 1248–1259, Apr. 2009.

[10] Y.-H. Liu and T.-H. Lin, "A Delta-Sigma Pulse-Width Digitization Technique for Super-Regenerative Receivers," *IEEE J. Solid-State Circuits*, vol. 45, no. 10, pp. 2066–2079, Oct. 2010.

[11] F. Sousa, et al., "A 20 mV Colpitts Oscillator Powered by a Thermoelectric Generator," *Proc. ISCAS*, pp. 2035-2038, 2012.

[12] Y.-C Shih and B.P. Otis, "An Inductorless DC–DC Converter for Energy Harvesting With a 1.2-μW Bandgap-Referenced Output Controller," *IEEE Trans. Circuits Syst. II*, vol. 58, no. 12, pp. 832–836, Dec. 2012.

[13] J. Bohorquez, et al., "Frequency-Domain Analysis of Super-Regenerative Amplifiers," *IEEE Trans. Microwave Theory and Techniques*, vol. 44, no. 4, pp. 1248–1259, Apr. 2009.

[14] UT1612MPR and UR1612MPR code specifications, http://www.spl-hk.com.hk/en/products.php?pname=UltrasonicSensor